JOURNAL OF VIROLOGY, Oct. 2002, p. 10356–10364 Vol. 76, No. 20
0022-538X/02/$04.00+0 DOI: 10.1128/JVI.76.20.10356–10364.2002

Role for Human Immunodeficiency Virus Type 1 Membrane Cholesterol in Viral Internalization

Mireille Guyader, Etsuko Kiyokawa,† Laurence Abrami, Priscilla Turelli, and Didier Trono*

Department of Genetics and Microbiology, University of Geneva, Geneva, Switzerland

Received 26 December 2001/Accepted 3 July 2002

The membrane of human immunodeficiency virus type 1 (HIV-1) virions contains high levels of cholesterol and sphingomyelin, an enrichment that is explained by the preferential budding of the virus through raft microdomains of the plasma membrane. Upon depletion of cholesterol from HIV-1 virions with methyl-β-cyclodextrin, infectivity was almost completely abolished. In contrast, this treatment had only a mild effect on the infectiousness of particles pseudotyped with the G envelope of vesicular stomatitis virus. The cholesterol-chelating compound nystatin had a similar effect. Cholesterol-depleted HIV-1 virions exhibited wild-type patterns of viral proteins and contained normal levels of cyclophilin A and glycosylphosphatidylinositol-anchored proteins. Nevertheless, and although they could still bind target cells, these virions were markedly defective for internalization. These results indicate that the cholesterol present in the HIV-1 membrane plays a prominent role in the fusion process that is key to viral entry and suggest that drugs capable of disturbing the lipid composition of virions could serve as a basis for the development of microbicides.

The lipid composition of the membrane of human immunodeficiency virus type 1 (HIV-1) differs significantly from that of the plasma membrane, displaying an unusually high content of cholesterol and sphingomyelin (5). HIV-1 particles also carry a number of cellular glycosylphosphatidylinositol (GPI)-anchored proteins on their surface (43) and in contrast lack molecules such as CD45 (40). This incorporation of particular cell membrane constituents is likely to be a direct consequence of the preferential budding of HIV-1 through so-called raft microdomains of the plasma membrane (40, 42).

Found in all mammalian cells, rafts are detergent-insoluble glycolipid- and cholesterol-enriched microdomains (also known as DIG or GEM), where GPI-anchored, doubly acylated and palmitoylated proteins are concentrated (for recent reviews, see references 9, 55, and 56). Rafts have been proposed to function as platforms for the assembly of membrane-associated macromolecular complexes that are at the heart of biological processes as diverse as signal transduction, T-cell activation, and virus budding (8, 9). Cholesterol plays a central function in these events in particular by maintaining sphingolipid rafts in a functional state, and its homeostasis is tightly regulated (10, 56).

Several membrane-associated HIV-1 proteins, including Nef, Gag, and Env, partition with rafts (40, 51, 65). While in the case of Gag this probably explains the site of virus budding (40, 42), the palmitoylation of the gp160 envelope glycoprotein of HIV-1 was recently shown to govern its raft association and to be critical for viral infectivity (51). The convergence of viral structural proteins in membrane microdomains thus appears to be important for particle assembly. In return, it is tempting to postulate that the resulting lipid composition of the viral membrane plays a role in some aspect of the viral life cycle. The results presented here indicate that this is indeed the case.

* Corresponding author. Mailing address: Department of Genetics and Microbiology, C. M. U., 1, rue Michel-Servet, 1211 Geneva 4, Switzerland. Phone: (41 22) 702 5720. Fax: (41 22) 702 5721. E-mail: didier.trono@medecine.unige.ch.

† Present address: Sphingolipid Functions Laboratory, Supra-Biomolecular System Research Group, RIKEN Frontier Research System, Saitama, Japan.

MATERIALS AND METHODS

Cells and viruses. HeLa P4 (14), HeLa P4-CCR5 (provided by O. Hartley, Geneva, Switzerland), and 293T cells were cultured in Dulbecco's modified Eagle's medium (DMEM) supplemented with 10% fetal calf serum. Single-round infectious assays were performed on the long terminal repeat (LTR)-*lacZ*-containing $CD4^+$ HeLa P4 cells derivatives as previously described (3). R9 is a full-length X4-tropic HIV-1 molecular clone (18). R8BaL is a full-length R5-tropic HIV-1 molecular clone in which the X4-tropic envelope of R9 has been replaced by the R5-tropic envelope of strain $HIV\text{-}1_{BaL}$.

Wild-type, envelope-defective, and vesicular stomatitis virus (VSV) G-pseudotyped viruses were prepared by transfection of 293T cells with R9 (or R8BaL), R9ΔEnv (62), and R9ΔEnv plus pMD.G (39), respectively. Virus-containing supernatants were subjected to low-speed centrifugation to remove cells and debris, filtered through a 0.45-μm nitrocellulose filter, and concentrated by ultracentrifugation at 26,000 rpm in an SW28 rotor for 90 min at 4°C. Viral pellets were resuspended in DMEM.

Wild-type, envelope-defective, and VSV G-pseudotyped green fluorescent protein (GFP)-labeled HIV-1 particles were prepared by transfection of 293T cells with R9 plus WXXF-GFP (63), R9ΔEnv plus WXXF-GFP, and R9ΔEnv plus pMD.G plus WXXF-GFP, respectively. Virus-containing supernatants were incubated with 10 mM methyl-β-cyclodextrin (Sigma-Fluka) or with phosphate-buffered saline (PBS) as a diluent control for 30 min at 37°C, loaded onto a 20% sucrose cushion, and ultracentrifuged at 26,000 rpm in an SW28 rotor for 90 min at 4°C. Virus stocks were normalized by their reverse transcriptase activity prior to infection.

To prepare cholesterol-depleted purified HIV-1 virions, concentrated virus stocks were incubated with 10 mM methyl-β-cyclodextrin or with PBS for 30 min at 37°C, cooled on ice, loaded onto a 20 to 60% sucrose gradient, and ultracentifuged at 24,000 rpm in an SW41 rotor for 16 h at 4°C. An aliquot of the harvested 1-ml fractions was lysed in 1% Triton for 30 min at 4°C and used to measure refraction index and reverse transcriptase activity. Pooled fractions corresponding to intact virions (peak of reverse transcriptase) were used to infect HeLa P4 (R9) or HeLa P4-CCR5 (R8BaL) cells.

For [^{3}H]cholesterol labeling of viruses, approximately 2×10^6 293T cells plated on a 10-cm-diameter dish were incubated for 12 h posttransfection with 50 μCi of [1α,2α-^{3}H]cholesterol in complete DMEM for an additional 24 h. Virus-containing supernatants were treated or not with cyclodextrin and purified by

ultracentrifugation through a 20% sucrose cushion at 13,000 rpm for 3 h at 4°C. The supernatant was lysed in 1% Triton, the viral pellet was resuspended in PBS–1% Triton, and radioactivity was quantified by scintillation counting. For nystatin treatment, viral supernatant were incubated with nystatin (Sigma-Fluka) or dimethyl sulfoxide as a diluent control for 30 min at 37°C, and viruses were purified by ultracentrifugation through a 20% sucrose cushion at 45,000 rpm in SW55 Beckman rotor for 1 h at 4°C.

Protein analysis. Viral protein analyses were performed on pooled sucrose gradient-purified virions, subjecting samples containing equivalent amounts of reverse transcriptase to 5% to 20% gradient sodium dodecyl sulfate-polyacrylamide gel electrophoresis (SDS-PAGE) followed by Western blotting with the following antibodies: cyclophilin A, anti-human cyclophilin A (Upstate Biotechnology Incorporated); matrix (MA) and integrase (IN), rabbit polyclonal antisera (19); capsid (CA), mouse monoclonal antibody (obtained through the National Institutes of Health AIDS Reagent Program from J. Allan); gp120, pool of two monoclonal antibodies (2342 and 2343, obtained through the National Institutes of Health AIDS Reagent Program from K. Ugen and D. Weiner); and gp41, mouse monoclonal antibody (provided by P. Cosson). The horseradish peroxidase-labeled secondary antibody was revealed by enhanced chemiluminescence (Amersham Pharmacia).

To examine the GPI-anchored protein content of virions, particles produced in Jurkat cells were either left untreated or incubated with methyl-β-cyclodextrin (10 mM, 30 min at 37°C) or phospholipase C (ICN Biomedical; 6 U/ml, 2 h at 37°C), purified by ultracentrifugation through a 20% sucrose, and analyzed by Western blot with proaerolysin and anti-proaerolysin antibodies as described (1).

Virus binding and internalization measurements. HeLa P4 cells were seeded at 2×10^5 cells/well in 12-well plates 24 h before infection. To measure attachment, cells were incubated for 1 h at 4°C before exposure to virus. Equivalent amounts of reverse transcriptase (corresponding to a multiplicity of infection of 0.1 for the wild-type virus) of gradient-purified virus were added to target cells at 4°C for 1 h, and cells were washed five times with ice-cold PBS and treated or not with 0.25% trypsin for 10 min at 37°C to remove surface-bound virus. After neutralization of the protease activity with fetal calf serum-containing DMEM, cells were washed twice with PBS and lysed in 200 μl of ice-cold PBS containing 0.5% Triton.

To measure internalization, the same conditions were used except that upon removal of unbound virus, cells were transferred to 37°C for 2 h before trypsin treatment and lysis as for the binding assay. At the end of each procedure, cell-associated virus was quantified by measuring the amount of p24 CA in the lysate by enzyme-linked immunosorbent assay (ELISA) (NEN Life Sciences).

Confocal microscopy. HeLa P4 cells were grown to 70% confluence on 12-mm-diameter glass coverslips in 12-well plates. To measure attachment, cells were incubated for 1 h at 4°C prior to virus exposure. Equivalent amounts of reverse transcriptase (corresponding to a multiplicity of infection of 1 for the wild-type virus) were added to target cells at 4°C for 1 h, cells were washed four times with ice-cold PBS–2% bovine serum albumin, labeled with tetramethylrhodamine-conjugated concanavalin A (TAMRA-ConA; Molecular Probes) for 2 min on ice, washed again four times, and fixed in 4% formaldehyde for 20 min at room temperature.

To measure internalization, virus was added to target cells at room temperature, and incubation was pursued at 37°C for 2 h. Cells were then washed four times with ice-cold PBS-2% bovine serum albumin and labeled with TAMRA-ConA as described above. When indicated, virus was added to target cells on ice in the presence of Texas Red-conjugated transferrin (Molecular Probes) to label endosomes. Incubation was performed at 37°C for either 20 min or 2 h, and cells were washed four times in PBS–2% bovine serum albumin and fixed in 4% formaldehyde for 20 min at room temperature.

CD4 labeling was performed on fixed cells with the CD4 antiserum 806 (obtained through the National Institutes of Health AIDS Research Program from R. Sweet) followed by an Alexa 568-conjugated secondary antibody. After washing in PBS, coverslips were secured to microscope slides with Mowiol as the mounting medium, and confocal microscopic analyses were performed on a confocal laser scanning fluorescence-inverted microscope (LSM 510; Zeiss). Each time, the two channels were recorded either together or independently to ensure the absence of interference between the channels. For each condition, we employed a Z stage motor to generate 12 to 16 cross-sectional planes of 0.4 μm in size on five different areas of each slide. The most representative sections are shown.

Monitoring of reverse transcription by PCR. The intracellular accumulation of HIV-1 reverse transcripts was monitored essentially as previously described (3), exposing 4×10^5 HeLa P4 cells to DNase I-treated gradient-purified viral stocks containing equivalent amounts of reverse transcriptase, corresponding to a multiplicity of infection of 0.1 for the control virus, in the presence of 50 μM azidothymidine (AZT) where indicated. At the indicated times postinfection, cells were washed three times in PBS, treated with 0.25% trypsin for 10 min at 37°C, washed twice more, and lysed with the DNeasy kit lysis buffer (Qiagen AG). PCR amplification was performed with HIV- and β-globin-specific primers as previously described (3).

RESULTS

Depletion of viral membrane cholesterol strongly decreases HIV-1 infectivity. As a first step towards investigating a potential role for the particular lipid composition of the HIV-1 membrane, we exposed purified virions to the drug methyl-β-cyclodextrin, known to extract cholesterol from membranes (46). Methyl-β-cyclodextrin was equally efficient at removing cholesterol from wild-type HIV-1 virions and from particles pseudotyped with VSV G (Fig. 1A). In both cases, incubation of [^{3}H]cholesterol-labeled virus with concentrations of methyl-β-cyclodextrin ranging from 2 to 20 mM led to a progressive loss of particle-associated [^{3}H]cholesterol, with a reciprocal increase in the amount of free [^{3}H]cholesterol released in the supernatant of pelleted virions (not shown).

We then measured the infectivity of the methyl-β-cyclodextrin-treated virions through a single-round assay with CD4$^+$ HeLa cells as the targets (Fig. 1B). For wild-type HIV-1, the drug-induced release of cholesterol correlated with a dramatic loss of infectivity. Incubation with 2 mM methyl-β-cyclodextrin, which removed between 10% and 20% of the virion-associated cholesterol (Fig. 1A), resulted in an 80 to 90% diminution in titer, and with 10 mM methyl-β-cyclodextrin, infectivity dropped by more than a hundredfold (Fig. 1B). Methyl-β-cyclodextrin had a strikingly less severe impact on the infectivity of VSV G-pseudotyped virions, with a mild decrease that stabilized at 25% of the control for 20 mM methyl-β-cyclodextrin. Treatment with 50 mM methyl-β-cyclodextrin led to complete loss of infectivity of VSV-pseudotyped HIV particles (data not shown), suggesting that, at this dose, methyl-β-cyclodextrin has deleterious consequences for virus stability and/or structure. Therefore, all subsequent experiments were performed with 10 mM methyl-β-cyclodextrin.

Since the infectivity of VSV G-pseudotyped virions was 10-fold higher than that of those bearing HIV-1 Env, one possibility to explain the mild effect of methyl-β-cyclodextrin treatment could be that higher concentrations of drug are required. In order to address this question, we produced VSV G-pseudotyped virions with an infectious titer comparable to that of HIV-1 virions by performing transfections with decreasing amounts of VSV G-expressing plasmid (Fig. 1C). In the experiment shown in Fig. 1C, we obtained a titer of 4.5×10^{-2} infectious units/cpm for HIV-1 virions and titers ranging from 2.7×10^{-2} to 1.8×10^{-3} infectious units/cpm for VSV G-pseudotyped HIV virions. Incubation with 10 mM methyl-β-cyclodextrin resulted in a 1.8- to 4.5-fold diminution in titer for VSV G-pseudotyped virions, whereas in similar conditions the infectivity of methyl-β-cyclodextrin-treated HIV-1 virions dropped by a thousandfold. These results showed that the dramatic effect of methyl-β-cyclodextrin treatment on HIV-1 infectivity is not due to its lower infectious potency compared to that of VSV G-pseudotyped particles.

When HIV virions were purified on a sucrose gradient after 10 mM methyl-β-cyclodextrin treatment, the inhibitory effect of the drug was confirmed for both X4 (R9)- and R5 (R8BaL)-

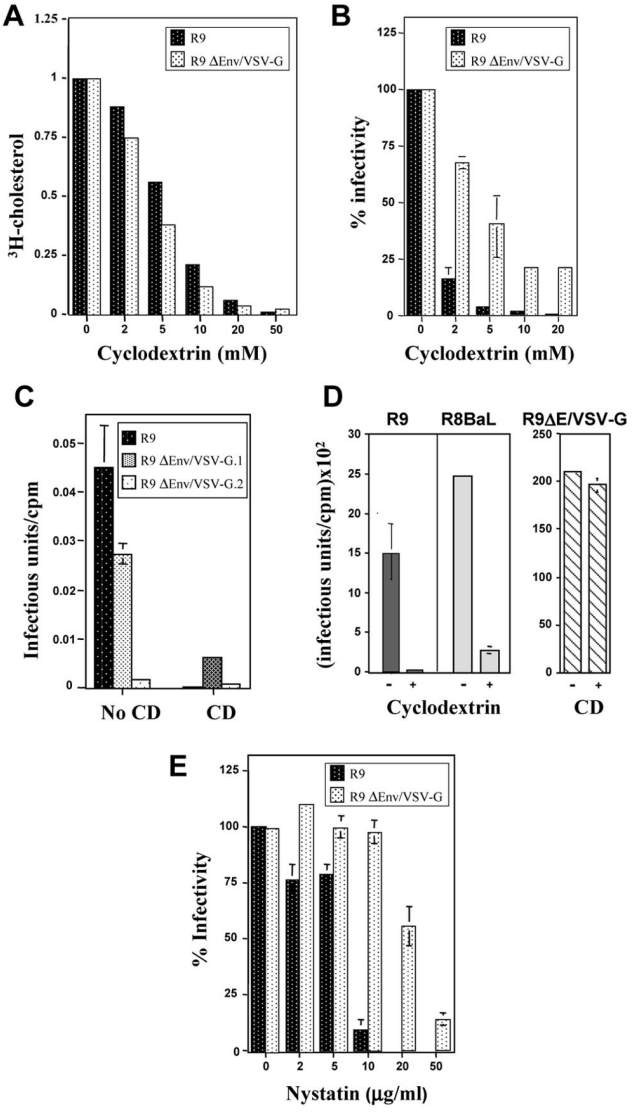

FIG. 1. Alteration of viral membrane cholesterol strongly decreases HIV-1 infectivity. (A and B) [^{3}H]cholesterol-labeled wild-type (R9) and VSV G-pseudotyped (R9ΔE/VSV G) virions were treated with increasing concentrations of methyl-β-cyclodextrin (CD). (A) Virions were subsequently concentrated by ultracentrifugation, and the amounts of pelletable and free [^{3}H]cholesterol were determined by scintillation counting. For "pellets," the numbers on the ordinate correspond to the ratio of pelleted to pelleted plus free cholesterol. (B) Infectivity of the above virions was determined in a single-round assay on CD4$^+$ HeLa P4 cells. Results are representative of at least five experiments. Infectivity of the untreated virus was given in each case the arbitrary value of 100%. (C) Infectivity of wild-type (R9) and VSV G-pseudotyped (R9ΔE/VSV G) virions produced by transfection with decreasing amounts of VSV G-expressing plasmid: 10 μg and 0.5 μg for R9ΔE/VSV G0.1 and R9ΔE/VSV G.2, respectively. Viral supernatants were treated or not with 10 mM methyl-β-cyclodextrin and concentrated by ultracentrifugation, and virion infectivity was determined on HeLa P4 cells. (D) Infectivity of control and cholesterol-depleted virions purified on a sucrose gradient after treatment with 10 mM methyl-β-cyclodextrin, expressed in infectious units per unit of reverse transcriptase activity. Infectivity of R9 and R9ΔE/VSV G virions was measured on HeLa P4 cells, while R8BaL virions were tested on HeLa P4-CCR5 cells. (E) Virus supernatants were treated with increasing concentrations of nystatin and purified by ultracentrifugation through a 20% sucrose cushion. Infectivity was determined as described for panel B.

tropic viruses (Fig. 1D). With this purification procedure, all effect of methyl-β-cyclodextrin on VSV G-pseudotyped virions was obliterated (Fig. 1D, right panel). This suggests that the small inhibition detected with less extensively purified material (Fig. 1B and 1C) reflected a nonspecific disruption of the virions at high methyl-β-cyclodextrin concentrations. Moreover, HIV-1 infectivity was also dramatically decreased when SupT1 CD4$^+$ lymphoid cells and primary T lymphocytes were used as targets (data not shown).

Incubation of HIV-1 virions with increasing concentrations of nystatin, a cholesterol-chelating agent known to disperse raft contents (50), also resulted in a dramatic reduction of HIV infectivity (Fig. 1E). As observed with methyl-β-cyclodextrin, nystatin had only a mild effect on VSV G-pseudotyped particles.

Cholesterol-depleted HIV-1 virions exhibit normal protein profiles. In order to examine further the effects of cyclodextrin on HIV-1 particles, we purified control and 10 mM methyl-β-cyclodextrin-treated virions on sucrose gradients and compared their density profiles and protein contents (Fig. 2). Methyl-β-cyclodextrin treatment of viral particles led to the release of some reverse transcriptase activity in the low-density fractions of the gradient, indicating that a portion of the virions were completely disrupted. However, for both control and methyl-β-cyclodextrin-treated samples, a prominent peak of reverse transcriptase activity was detected at a density between 1.14 and 1.18 g/ml, typical of HIV-1 virions (Fig. 2A).

The same kind of pattern was observed in the density profiles of sucrose gradient-purified methyl-β-cyclodextrin-treated M-tropic and VSV G-pseudotyped HIV-1 particles (not illustrated). When we analyzed the peak fractions of the gradients by Western blotting with various antibodies (Fig. 2B), we detected no difference between control and methyl-β-cyclodextrin-treated virions in all the major viral proteins, including Env (gp120 and gp41), IN, CA, and MA. Methyl-β-cyclodextrin-treated virions also contained wild-type amounts of cyclophilin A, a cellular protein that is recruited in virions by CA (17, 60).

GPI-anchored proteins preferentially associate with the lipid raft microdomains of the plasma membrane and as a consequence decorate the surface of outgoing HIV-1 particles (40). The removal of membrane cholesterol by methyl-β-cyclodextrin can induce the release of GPI-anchored molecules from the surface of murine T lymphocytes (21). This suggested that the methyl-β-cyclodextrin treatment of HIV-1 virions could similarly affect their GPI-linked protein content. We addressed this possibility by Western blot analysis, using as a probe the bacterial protoxin proaerolysin, which specifically binds to the glycosyl moiety of GPI-anchored proteins (1, 2, 15) (Fig. 2C). No significant difference was detected between control and methyl-β-cyclodextrin-treated virions in this assay either. Importantly, the proaerolysin-mediated signal was completely eliminated after treating virions with phospholipase C, an enzyme that cleaves the GPI anchor. Finally, electron microscopy analyses did not reveal any significant difference between methyl-β-cyclodextrin-treated and control virions (data not shown).

Cholesterol-depleted HIV-1 particles are defective for internalization. Viral entry is a multistep process that involves the binding of the viral particle to the cell surface, the fusion of the

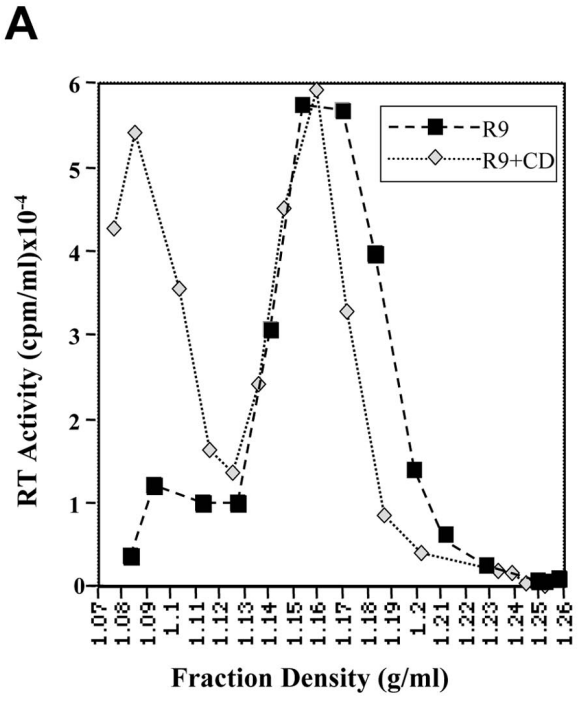

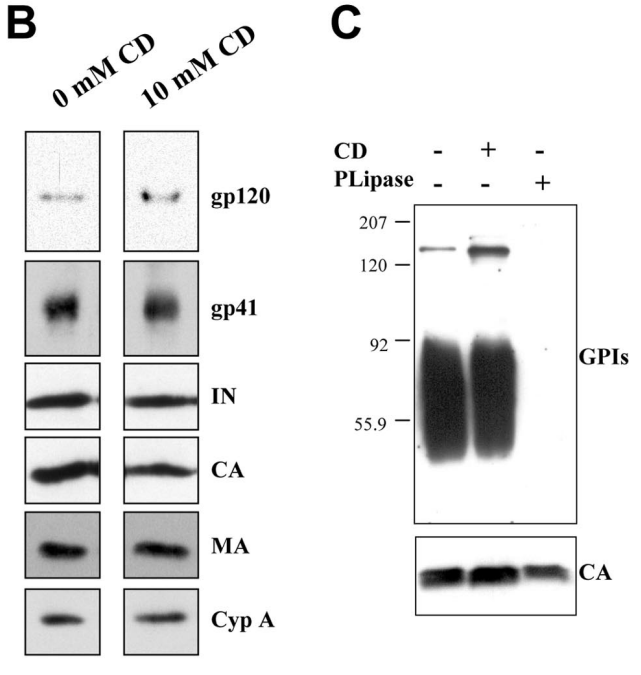

FIG. 2. Cholesterol-depleted purified particles exhibit normal protein profile. (A) Reverse transcriptase (RT) activity in sucrose density gradient fractions of native and methyl-β-cyclodextrin-treated R9 HIV-1 virions. (B) Immunoblot analysis with the indicated antisera of pooled fractions corresponding to intact virions of untreated (0 mM methyl-β-cyclodextrin [CD]) and methyl-β-cyclodextrin-treated (10 mM methyl-β-cyclodextrin) R9. Cyp A, cyclophilin A. (C) GPI-anchored protein profile of untreated, methyl-β-cyclodextrin-treated, and phospholipase C (PLipase)-treated virions with the proaerolysin/anti-proaerolysin overlay procedure (top). The same membrane was probed by Western blotting with an anti-CA antibody (bottom).

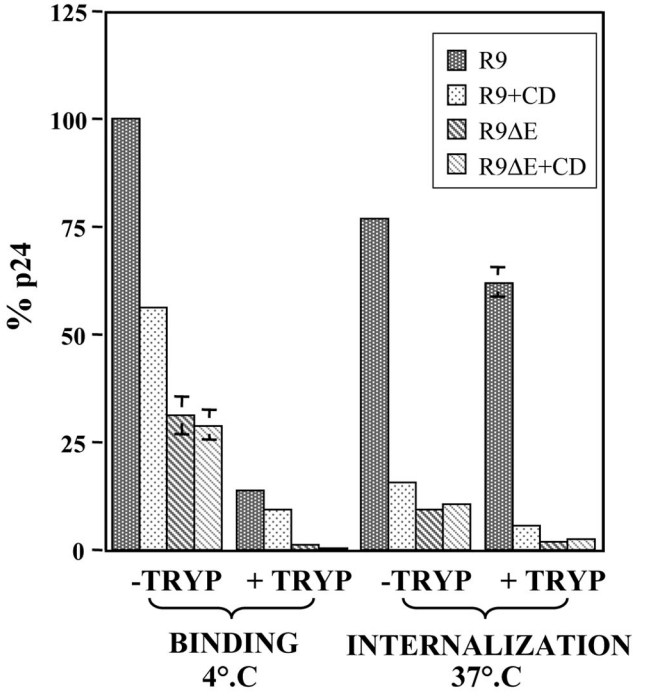

FIG. 3. Cholesterol-depleted particles show a strong internalization defect. Virus attachment and internalization measured on HeLa P4 cells for wild-type (R9) and envelope-defective (R9ΔE) viruses after treatment of the virions with cyclodextrin (CD) where indicated. Results are representative of four independent experiments. The multiplicity of infection was 0.1. After binding (at 4°C) or internalization (at 37°C), cells were exposed to trypsin (+TRYP) or to PBS (−TRYP). The amount of cell-associated p24 after incubation with wild-type virus at 4°C was given the arbitrary value of 100%.

viral and cellular membranes, and finally the delivery of the viral inner components into the cytoplasm of the target cell. In order to determine whether viral membrane cholesterol plays a role in this sequence of events, we first used a modified version of an entry assay that dissects binding and fusion (52). Two studies have reported that when target cells are exposed to high doses of HIV, a significant fraction of virions are internalized by endocytosis and are subsequently degraded (35, 53). In order to minimize background due to this nonspecific process, infections were performed at a multiplicity of infection of 0.1. Virus attachment was measured at 4°C, a temperature at which both membrane fusion and endocytosis are very ineffective; virus internalization was then examined by incubating the virus-cell mixture at 37°C. In either case, trypsin was used to remove virions that were surface bound but not internalized. $CD4^+$ HeLa cells served as targets, and an envelope-defective mutant (R9ΔE) was included as a negative control, the values for which could be subtracted from those obtained with the test viruses and represented the extent of nonspecific endocytosis in our assay conditions.

Methyl-β-cyclodextrin treatment induced an approximately 2.5-fold decrease in the ability of HIV-1 particles to bind target cells, indicating that it only slightly perturbed the ability of the viral envelope to interact with its cell surface receptors (Fig. 3). The cholesterol-depleted virions, however, were markedly de-

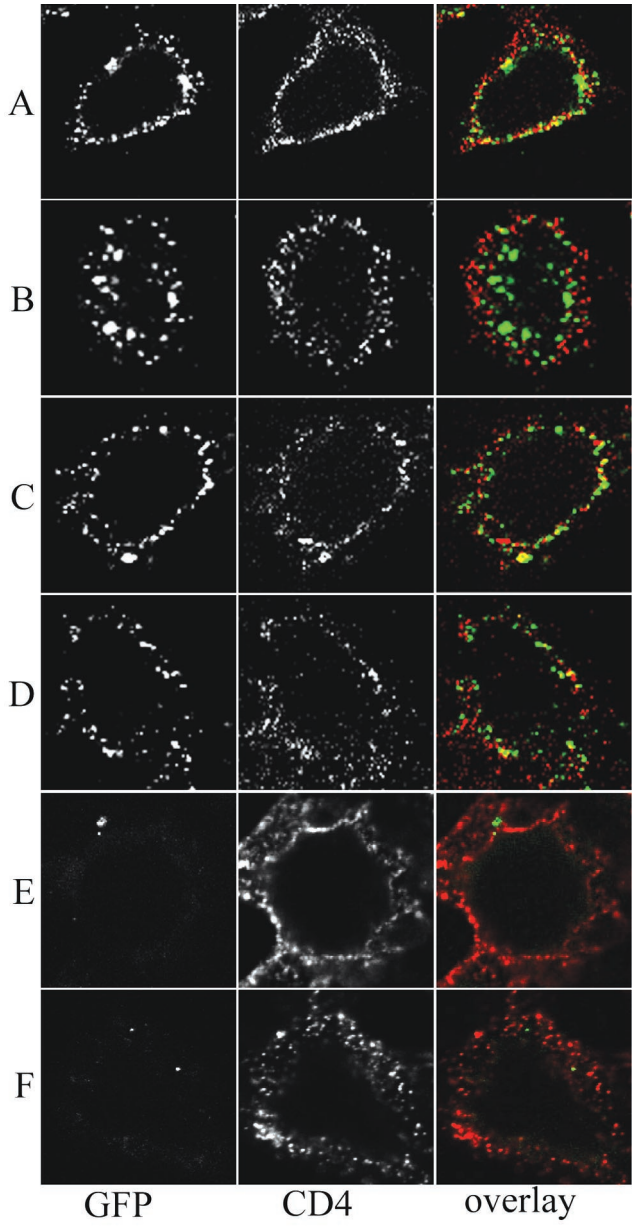

FIG. 4. Confocal microscopic analysis of virus attachment and internalization. GFP-labeled wild-type (A and B), methyl-β-cyclodextrin-treated (C and D), and envelope-defective (E and F) viruses were used to infect $CD4^+$ HeLa cells. Inocula contained equivalent amounts of reverse transcriptase corresponding to a multiplicity of infection of 1 for the wild-type untreated control. (A, C, and E) Virus attachment, assessed after incubating the virus with the cells at 4°C for 1 h. (B, D, and F) Virus internalization, examined after 2 h at 37°C. CD4 staining (red) was performed after fixation and without permeabilization to label only molecules present at the cell surface.

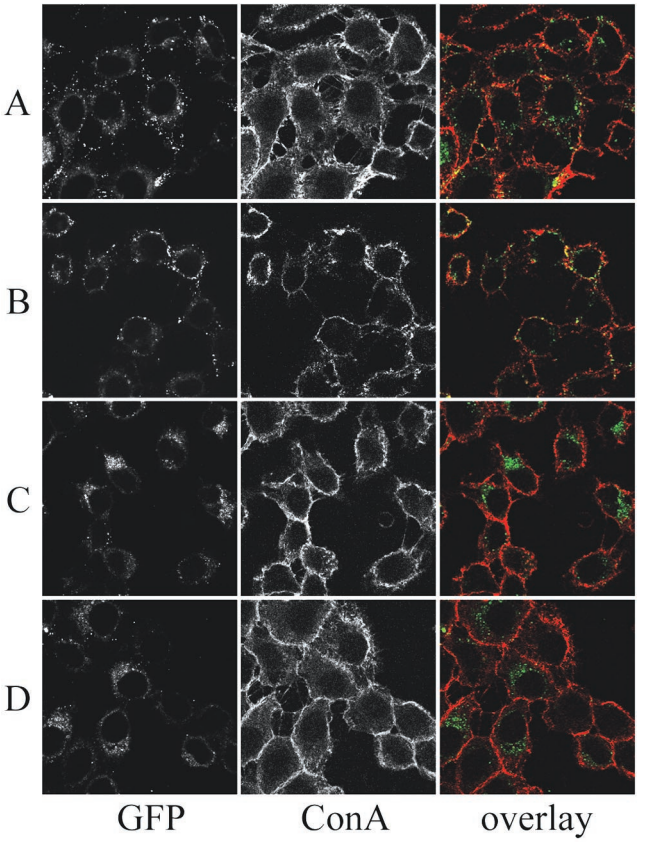

FIG. 5. Confocal microscopic analysis of intracellular virus. GFP-labeled wild-type (A) and methyl-β-cyclodextrin-treated (B) HIV-1 particles and R9ΔE/VSV G (C) and methyl-β-cyclodextrin-treated R9ΔE/VSV G (D) viruses were used to infect $CD4^+$ HeLa cells. Inocula contained equivalent amounts of reverse transcriptase corresponding to a multiplicity of infection of 1 for the wild-type untreated control. Virus internalization was examined after 2 h at 37°C. TAMRA-ConA was used to stain cell membranes.

fective for internalization, with less than 5% residual activity compared with the untreated virus.

To illustrate further the defect in internalization observed with cholesterol-depleted HIV particles, we analyzed the binding and internalization of GFP-labeled virions by confocal microscopy (Fig. 4, 5 and 6). For this, viruses were produced from cells expressing a GFP derivative carrying a Vpr-binding tag, allowing the incorporation of this fusion protein into the viral particles and the subsequent visualization of internalized viral nucleoprotein complexes by confocal microscopy, as described previously (63).

In a first set of experiments, wild-type, methyl-β-cyclodextrin-treated, and envelope-defective HIV viruses were tested in parallel with $CD4^+$ HeLa cells as targets. Inocula contained equivalent amounts of reverse transcriptase for each virus, corresponding to a multiplicity of infection of 1 for the untreated wild type. Virus attachment was examined at 4°C, while virus entry was monitored after 2 h of incubation at 37°C. After fixation with formaldehyde, a CD4-specific antibody was used to stain receptor molecules associated with the cell surface.

When infection was performed at 4°C, both cholesterol-depleted and control particles were detected at the cell membrane, partly colocalizing with CD4 (Fig. 4A and 4C). At 37°C, wild-type-infected cells exhibited prominent intracellular green spots, corresponding to internalized viral nucleoprotein complexes (Fig. 4B). In contrast, with cholesterol-depleted particles, small green dots were detected almost exclusively at the cell periphery, with very little intracellular GFP signal (Fig. 4D). The control envelope-defective virus induced a minimal degree of fluorescent signal after infection at either 4 or 37°C

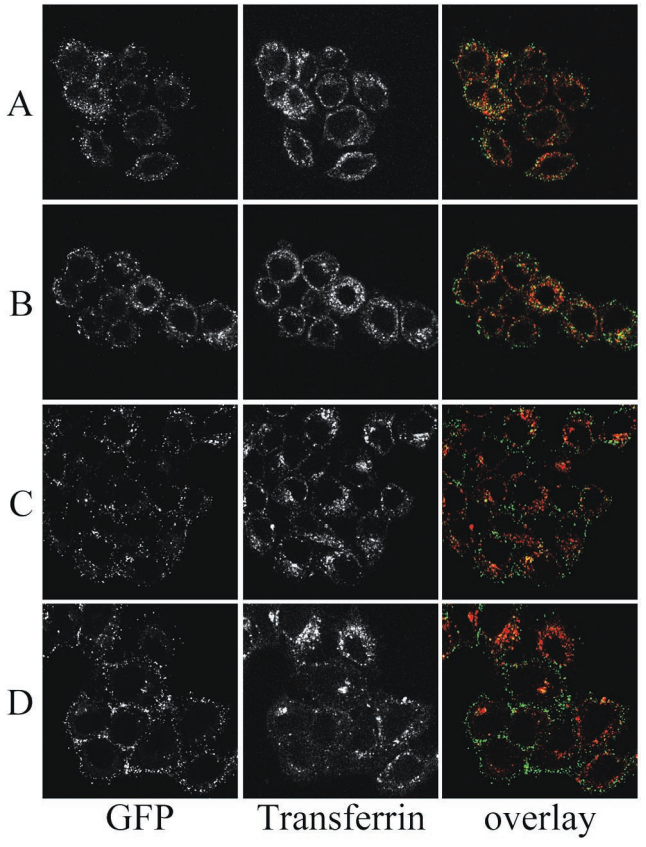

FIG. 6. Assessment of viral endocytosis. GFP-labeled wild-type R9ΔE/VSV G (A), methyl-β-cyclodextrin-treated R9ΔE/VSV G (B), wild-type HIV-1 (C), and methyl-β-cyclodextrin-treated HIV-1 (D) viruses were used to infect $CD4^+$ HeLa cells. Inocula contained equivalent amounts of reverse transcriptase corresponding to a multiplicity of infection of 10 for the wild-type untreated control. Virus internalization was performed in the presence of Texas Red-conjugated transferrin to label endosomes and examined after 20 min (A and B) or 2 h (C and D) at 37°C.

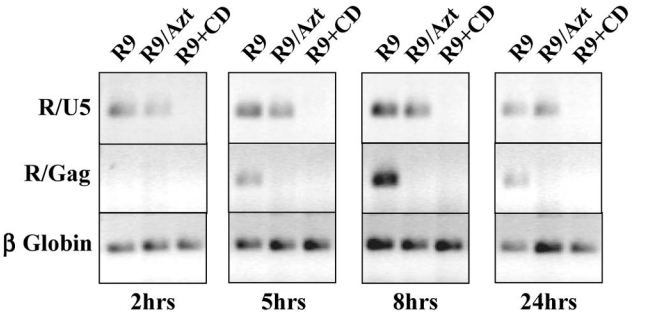

FIG. 7. PCR-based monitoring of reverse transcription. HeLa P4 cells were infected with wild-type HIV-1 in the absence (R9) or presence (R9/AZT) of AZT or with cholesterol-depleted (R9+CD) virus. The R/U5 primer pair amplifies the minus-strand strong-stop DNA, while R/Gag detects late products generated after the second template switch. β-Globin primers were used as a control to monitor the cellular DNA content of lysate samples.

(Fig. 4E and 4F). With this virus, multiplicities of infection of at least 100 had to be used to recover an intracellular signal (not illustrated), confirming that nonspecific virion endocytosis did not significantly affect our results.

A second set of experiments were also performed, testing in parallel wild-type HIV-1 or VSV G-pseudotyped particles, with or without methyl-β-cyclodextrin treatment, and envelope-defective viruses as negative controls, with the same targets as in Fig. 4 (Fig. 5 and 6). First, TAMRA-ConA was used to label the cell surface (Fig. 5). As already observed in Fig. 4, when infections were performed at 4°C, both control and cholesterol-depleted particles were detected at the cell membrane (data not shown). At 37°C, cells exposed to wild-type HIV-1 exhibited prominent intracellular fluorescent dots (Fig. 5A), whereas with cholesterol-depleted particles, the GFP signal was detected mostly at the cell periphery and minimally inside the cells (Fig. 5B). When cells were infected with VSV G-pseudotyped virions, GFP fluorescent spots were prominent in the cell cytoplasm, with or without prior methyl-β-cyclodextrin treatment (Fig. 5C and 5D).

To examine further the potential interference of nonspecific endocytosis with our assay, virus internalization was examined at a higher multiplicity of infection (10 infectious units per cell) in the presence of Texas Red-conjugated transferrin to label endosomes (Fig. 6). Internalization was extremely rapid with VSV G-pseudotyped particles, inducing a strong intracellular GFP signal that was visible after only 20 min, whether or not methyl-β-cyclodextrin had been used (Fig. 6A and 6B). With this virus, similar images were obtained after 2 h (data not shown). Based on the analysis of four independent Z stacks containing an average of 10 cells per stack, the percentage of GFP molecules colocalizing with transferrin at 20 min was 29.15% (± 5.52%) and 34.35% (± 12.71%) for wild-type and methyl-β-cyclodextrin-treated VSV G-pseudotyped virions, respectively. These values suggest that cyclodextrin treatment had no impact on the ability of VSV G-pseudotyped virions to enter target cells by endocytosis.

With the wild-type HIV-1 virions, very few GFP-labeled particles were detected inside the cells after 20 min (data not shown). At 2 h, the intracellular virus-specific signal was prominent for the untreated virus (Fig. 6C) and less important for the methyl-β-cyclodextrin-treated virions, which remained mostly peripheral (Fig. 6D). Still, in both cases, some intracellular virus colocalizing with transferrin was observed. Based on the analysis of seven independent Z stacks containing an average of eight cells per stack, the percentage of colocalization between the GFP and transferrin signals was 17.14% (± 8.07%) and 26.68% (± 5.58%) of the total signal for the wild-type and methyl-β-cyclodextrin-treated HIV-1 virions, respectively. Thus, with cholesterol depletion, nonspecific endocytosis is not only not prevented, but also ends up representing a greater proportion of the total virus-specific signal.

To ascertain that the loss of infectivity of methyl-β-cyclodextrin-treated HIV-1 resulted from an entry problem, we monitored by PCR the synthesis of viral reverse transcripts in newly infected cells (Fig. 7). At 2 h postinfection, wild-type-infected cells exhibited readily detectable levels of minus-strand strong-stop DNA, the earliest product of reverse transcription amplified here by the R/U5 primer pair. At 5 h postinfection, these cells further started to accumulate late reverse transcripts synthesized after the second of the two reverse transcriptase tem-

plate switches leading to proviral DNA synthesis, amplified here by the R/Gag primer pair. At 24 h, there was a slight decrease in the total amount of viral DNA in wild-type-infected cells, consistent with previous observations (25). This decrease probably reflects the degradation of at least some unintegrated DNA (25). In cells exposed to the cholesterol-depleted virus and up to 24 h postinfection, no viral DNA was detectable.

AZT treatment of wild-type-infected cells prevented the synthesis of elongated reverse transcripts, confirming that these products reflected de novo reverse transcription. However, AZT did not affect the levels of minus-stand strong-stop DNA, either because this particular DNA species was already present in the virions (30, 61) or because AZT is a chain terminator, the inhibitory effect of which is directly proportional to the length of the synthesized DNA and hence has little impact on very short reverse transcriptase products. In either case, the finding of early reverse transcripts in wild-type-infected cells but not in cells exposed to cholesterol-depleted virions confirms that the latter virus fails to enter its targets productively.

DISCUSSION

The HIV-1 envelope glycoprotein (Env) comprises a receptor-binding surface moiety, gp120, noncovalently associated to a fusogenic transmembrane protein, gp41, both assembled in trimers. Env mediates HIV-1 entry, which can be divided into three steps. First, the virus attaches to the cell surface through the recognition and binding of specific cell surface receptors, in particular CD4, by gp120. After a structural modification of gp120 allowing the engagement of a coreceptor (most commonly the CCR5 or CXCR4 chemokine receptors), a conformational change is triggered in gp41, revealing its fusogenic potential. Finally, the viral and cellular membranes fuse with each other to deliver the virion inner components into the cytoplasm (16).

Here, we present a series of evidence demonstrating that HIV-1 entry critically depends on the high cholesterol content of the viral membrane, itself the result of the selective budding of this virus through lipid rafts. Following treatment with membrane cholesterol-extracting drugs such as methyl-β-cyclodextrin, HIV-1 virions could still bind target cells but could not be internalized. We did not succeed in consistently reintroducing the cholesterol in the membrane of methyl-β-cyclodextrin-treated HIV-1 particles, which would have helped ascertain that the loss of this lipid was solely responsible for this defective phenotype. However, biochemical and ultrastructural analyses revealed that the treated virions did not present obvious defects in their structure and protein content. Furthermore, the conserved infectivity of the methyl-β-cyclodextrin- or nystatin-treated VSV G-pseudotyped virus indicates that these drugs did not cause a disruption of the virions and inhibited no replication step other than viral entry. Our results are in agreement with the recent study of Zheng et al., who showed that Nef increases virion infectivity in a manner that depends on cholesterol and GM1 in lipid rafts (70), and confirm the previously described importance of rafts in HIV-1 infectivity (29, 42).

How to explain the cholesterol requirement for HIV-1 entry? Cholesterol depletion of HIV-1 virions does not significantly affect the virus's ability to bind target cells. It could thus be that the gp41 conformational change that initiates fusion is critically affected by the lipid composition of the membrane holding the membrane-spanning domain of Env. In particular, the triple coiled-coil, six-helix bundle structure that results from the juxtaposition of three gp41 "fusion peptides" and whose formation is rate limiting for fusion may be stabilized in the context of a cholesterol-rich, highly organized lipid bilayer (12, 38, 66). Furthermore, membrane fusion is a cooperative process, and it is currently estimated that four to six coreceptors (27), multiple CD4 molecules (28), and from three to six Env trimers are needed to form a fusion pore. The lateral movements of Env implied by this model, with a possible "capping" of the virus at the virus-cell interface by juxtaposed Env trimers, may be facilitated in the context of a membrane that contains a high cholesterol/phospholipid ratio.

By analogy, cyclodextrin-induced cholesterol depletion of target cell membrane has been shown to inhibit HIV entry (29, 33), and this blockade correlated with a loss of the gp120-induced lateral association of CD4 and CXCR4 (33). A similar type of requirement may apply to the viral membrane. Finally, the altered fluidity of the cholesterol-depleted viral membrane could prevent its fusion with the cell membrane in spite of a successful deployment of the gp41 fusion peptide. It could be argued that the minimal effect of cholesterol depletion on the infectivity of HIV (VSV G) pseudotypes and on their efficiency of entry into target cells makes this last hypothesis less likely. However, in this case, fusion occurs in the endosome, where requirements may differ somewhat.

A recent study found that the infectivity of Moloney murine leukemia virus was more severely affected by cholesterol depletion when the particles were coated with VSV G than with the ecotropic envelope protein (45). Although Moloney murine leukemia virus and HIV may have distinct requirements, we note that in this other study, methyl-β-cyclodextrin treatment was performed on producer cells and not on viral particles, drug concentrations (up to 2.5 mM) were lower than in our experiments, and virions were not gradient purified. Here, we found that the infectivity of gradient-purified methyl-β-cyclodextrin-treated VSV G-pseudotyped HIV particles did not differ significantly from that of untreated virus.

While a number of studies have examined the importance of the lipid composition of target cell membranes in the entry of various enveloped viruses (4, 6, 7, 20, 23, 31, 41, 59, 67), this question has seldom been directed at the viral membrane. The lipid composition of viral membranes has been the focus of extensive investigations and for a number of viruses, including retroviruses, has been shown to differ from that of the host plasma membrane ((37, 44, 47, 48, 58; reviewed in reference 4). Lipid rafts likely constitute the preferential site of assembly and release of several enveloped viruses besides HIV-1, including orthomyxoviruses such as influenza virus (54, 69) and paramyxoviruses such as measles virus (34, 64). Plasma membrane cholesterol is also important for the budding of alphaviruses like Semliki Forest virus and Sindbis virus (31, 32, 36).

Very recently, Bavari et al. identified rafts as the gateways for the entry and exit of filoviruses such as Ebola and Marburg viruses (6). It is therefore noteworthy that influenza virus, the paramyxoviruses, and Ebola virus use the same fusion mechanism as HIV-1, all having envelope glycoproteins that form

six-helix bundles bringing the fusion peptide (and the cellular membrane) in close proximity to the transmembrane domain (and the viral membrane) (reviewed in references 13 and 57). Based on these similarities, it would be interesting to test whether entry of these other viruses also depends on the presence of cholesterol in their lipid bilayer.

Peptides and small-molecule inhibitors that block viral fusion by interfering with the conformational change of gp41 to a fusion-active state have recently been described (11, 22, 26, 49, 68). One such peptide, termed T20, has been shown to reduce virus loads significantly in vivo and is currently in clinical trials (24). By analogy, the results of the present study raise the interesting possibility that drugs affecting the metabolism of cholesterol might represent useful complements to currently available antiviral therapies. The systemic administration of drugs extracting membrane cholesterol could pose important toxicity problems unless compounds that preferentially alter viral rather than cellular membranes can be identified. However, the topical administration of such drugs may be less problematic, implying that cholesterol-depleting substances could serve as bases for the development of microbicides. In that respect, the ability of nystatin to abolish HIV infectivity is remarkable, because this polyene antibiotic has been used successfully for many years for the topical treatment of vaginal candidiasis. It may well be that its use or that of functionally related compounds could be redirected to the prevention of sexual HIV transmission. Testing this hypothesis in an animal model such as the simian immunodeficiency virus-rhesus macaque system is an obvious next step, the result of which might open new perspectives for HIV prophylaxis.

ACKNOWLEDGMENTS

We thank G. van der Goot, M. Fivaz, P. Cosson, and O. Hartley for the kind gift of reagents and for helpful discussions; R. Stalder and N. Demaurex for help with the confocal microscopy; and M. Loche for the artwork.

This study was supported by the Swiss National Science Foundation, the Gabriella Giorgi-Cavaglieri Foundation, the Dormeur Foundation, and the National Institutes of Health (D.T.); the Japanese Foundation for AIDS Prevention (E.K.); the Human Frontier Science Program (P.T.); and the INSERM (M.G.).

REFERENCES

1. **Abrami, L., M. Fivaz, P. E. Glauser, R. G. Parton, and F. G. van der Goot.** 1998. A pore-forming toxin interacts with a GPI-anchored protein and causes vacuolation of the endoplasmic reticulum. J. Cell Biol. **140:**525–540.
2. **Abrami, L., M. C. Velluz, Y. Hong, K. Ohishi, A. Mehlert, M. Ferguson, T. Kinoshita, and F. Gisou van der Goot.** 2002. The glycan core of GPI-anchored proteins modulates aerolysin binding but is not sufficient: the polypeptide moiety is required for the toxin-receptor interaction. FEBS Lett. **512:**249–254.
3. **Aiken, C., and D. Trono.** 1995. Nef stimulates human immunodeficiency virus type 1 proviral DNA synthesis. J. Virol. **69:**5048–5056.
4. **Aloia, R. C., C. C. Curtain, and F. C. Jensen.** 1992. Membrane cholesterol and human immunodeficiency virus infectivity. Adv. Membrane Fluidity **6:** 283–304.
5. **Aloia, R. C., H. Tian, and F. C. Jensen.** 1993. Lipid composition and fluidity of the human immunodeficiency virus envelope and host cell plasma membranes. Proc. Natl. Acad. Sci. USA **90:**5181–5185.
6. **Bavari, S., C. M. Bosio, E. Wiegand, G. Ruthel, A. B. Will, T. W. Geisbert, M. Hevey, C. Schmaljohn, A. Schmaljohn, and M. J. Aman.** 2002. Lipid raft microdomains: a gateway for compartmentalized trafficking of Ebola and Marburg viruses. J. Exp. Med. **195:**593–602.
7. **Bron, R., J. M. Wahlberg, H. Garoff, and J. Wilschut.** 1993. Membrane fusion of Semliki Forest virus in a model system: correlation between fusion kinetics and structural changes in the envelope glycoprotein. EMBO J. **12:**693–701.
8. **Brown, D. A., and E. London.** 1998. Functions of lipid rafts in biological membranes. Annu. Rev. Cell Dev. Biol. **14:**111–136.
9. **Brown, D. A., and E. London.** 2000. Structure and function of sphingolipid- and cholesterol-rich membrane rafts. J. Biol. Chem. **275:**17221–17224.
10. **Brown, D. A., and E. London.** 1998. Structure and origin of ordered lipid domains in biological membranes. J. Membr. Biol. **164:**103–114.
11. **Chan, D. C., C. T. Chutkowski, and P. S. Kim.** 1998. Evidence that a prominent cavity in the coiled coil of HIV type 1 gp41 is an attractive drug target. Proc. Natl. Acad. Sci. USA **95:**15613–15617.
12. **Chan, D. C., D. Fass, J. M. Berger, and P. S. Kim.** 1997. Core structure of gp41 from the HIV envelope glycoprotein. Cell **89:**263–273.
13. **Chan, D. C., and P. S. Kim.** 1998. HIV entry and its inhibition. Cell **93:**681–684.
14. **Charneau, P., G. Mirambeau, P. Roux, S. Paulous, H. Buc, and F. Clavel.** 1994. HIV-1 reverse transcription. A termination step at the center of the genome. J. Mol. Biol. **241:**651–662.
15. **Diep, D. B., K. L. Nelson, S. M. Raja, E. N. Pleshak, and J. T. Buckley.** 1998. Glycosylphosphatidylinositol anchors of membrane glycoproteins are binding determinants for the channel-forming toxin aerolysin. J. Biol. Chem. **273:**2355–2360.
16. **Doms, R. W., and D. Trono.** 2000. The plasma membrane as a combat zone in the HIV battlefield. Genes Dev. **14:**2677–2688.
17. **Franke, E. K., H. E. Yuan, and J. Luban.** 1994. Specific incorporation of cyclophilin A into HIV-1 virions. Nature **372:**359–362.
18. **Gallay, P., T. Hope, D. Chin, and D. Trono.** 1997. HIV-1 infection of nondividing cells through the recognition of integrase by the importin/karyopherin pathway. Proc. Natl. Acad. Sci. USA **94:**9825–9830.
19. **Gallay, P., S. Swingler, J. Song, F. Bushman, and D. Trono.** 1995. HIV nuclear import is governed by the phosphotyrosine-mediated binding of matrix to the core domain of integrase. Cell **83:**569–576.
20. **Hug, P., H. M. Lin, T. Korte, X. Xiao, D. S. Dimitrov, J. M. Wang, A. Puri, and R. Blumenthal.** 2000. Glycosphingolipids promote entry of a broad range of human immunodeficiency virus type 1 isolates into cell lines expressing CD4, CXCR4, and/or CCR5. J. Virol. **74:**6377–6385.
21. **Ilangumaran, S., and D. C. Hoessli.** 1998. Effects of cholesterol depletion by cyclodextrin on the sphingolipid microdomains of the plasma membrane. Biochem. J. **335:**433–440.
22. **Jiang, S., K. Lin, N. Strick, and A. R. Neurath.** 1993. HIV-1 inhibition by a peptide. Nature **365:**113.
23. **Kielian, M. C., and A. Helenius.** 1984. Role of cholesterol in fusion of Semliki Forest virus with membranes. J. Virol. **52:**281–283.
24. **Kilby, J. M., S. Hopkins, T. M. Venetta, B. DiMassimo, G. A. Cloud, J. Y. Lee, L. Alldredge, E. Hunter, D. Lambert, D. Bolognesi, T. Matthews, M. R. Johnson, M. A. Nowak, G. M. Shaw, and M. S. Saag.** 1998. Potent suppression of HIV-1 replication in humans by T-20, a peptide inhibitor of gp41-mediated virus entry. Nat. Med. **4:**1302–1307.
25. **Kim, S. Y., R. Byrn, J. Groopman, and D. Baltimore.** 1989. Temporal aspects of DNA and RNA synthesis during human immunodeficiency virus infection: evidence for differential gene expression. J. Virol. **63:**3708–3713.
26. **Kliger, Y., S. A. Gallo, S. G. Peisajovich, I. Munoz-Barroso, S. Avkin, R. Blumenthal, and Y. Shai.** 2001. Mode of action of an antiviral peptide from HIV-1. Inhibition at a post-lipid mixing stage. J. Biol. Chem. **276:**1391–1397.
27. **Kuhmann, S. E., E. J. Platt, S. L. Kozak, and D. Kabat.** 2000. Cooperation of multiple CCR5 coreceptors is required for infections by human immunodeficiency virus type 1. J. Virol. **74:**7005–7015.
28. **Layne, S. P., M. J. Merges, M. Dembo, J. L. Spouge, and P. L. Nara.** 1990. HIV requires multiple gp120 molecules for CD4-mediated infection. Nature **346:**277–279.
29. **Liao, Z., L. M. Cimakasky, R. Hampton, D. H. Nguyen, and J. E. Hildreth.** 2001. Lipid rafts and HIV pathogenesis: host membrane cholesterol is required for infection by HIV type 1. AIDS Res. Hum. Retroviruses **17:**1009–1019.
30. **Lori, F., F. di Marzo Veronese, A. L. de Vico, P. Lusso, M. S. Reitz, and R. C. Gallo.** 1992. Viral DNA carried by human immunodeficiency virus type 1 virions. J. Virol. **66:**5067–5074.
31. **Lu, Y. E., T. Cassese, and M. Kielian.** 1999. The cholesterol requirement for Sindbis virus entry and exit and characterization of a spike protein region involved in cholesterol dependence. J. Virol. **73:**4272–4278.
32. **Lu, Y. E., and M. Kielian.** 2000. Semliki forest virus budding: assay, mechanisms, and cholesterol requirement. J. Virol. **74:**7708–7719.
33. **Manes, S., G. del Real, R. A. Lacalle, P. Lucas, C. Gomez-Mouton, S. Sanchez-Palomino, R. Delgado, J. Alcami, E. Mira, and A. C. Martinez.** 2000. Membrane raft microdomains mediate lateral assemblies required for HIV-1 infection. EMBO Rep. **1:**190–196.
34. **Manie, S. N., S. Debreyne, S. Vincent, and D. Gerlier.** 2000. Measles virus structural components are enriched into lipid raft microdomains: a potential cellular location for virus assembly. J. Virol. **74:**305–311.
35. **Marechal, V., F. Clavel, J. M. Heard, and O. Schwartz.** 1998. Cytosolic Gag p24 as an index of productive entry of human immunodeficiency virus type 1. J. Virol. **72:**2208–2212.
36. **Marquardt, M. T., T. Phalen, and M. Kielian.** 1993. Cholesterol is required in the exit pathway of Semliki Forest virus. J. Cell Biol. **123:**57–65.
37. **McSharry, J. J., and R. R. Wagner.** 1971. Lipid composition of purified vesicular stomatitis viruses. J. Virol. **7:**59–70.

38. **Melikyan, G. B., R. M. Markosyan, H. Hemmati, M. K. Delmedico, D. M. Lambert, and F. S. Cohen.** 2000. Evidence that the transition of HIV-1 gp41 into a six-helix bundle, not the bundle configuration, induces membrane fusion. J. Cell Biol. **151:**413–423.
39. **Naldini, L., U. Blomer, P. Gallay, D. Ory, R. Mulligan, F. H. Gage, I. M. Verma, and D. Trono.** 1996. In vivo gene delivery and stable transduction of nondividing cells by a lentiviral vector. Science **272:**263–267.
40. **Nguyen, D. H., and J. E. Hildreth.** 2000. Evidence for budding of human immunodeficiency virus type 1 selectively from glycolipid-enriched membrane lipid rafts. J. Virol. **74:**3264–3272.
41. **Niyogi, K., and J. E. Hildreth.** 2001. Characterization of new syncytium-inhibiting monoclonal antibodies implicates lipid rafts in human T-cell leukemia virus type 1 syncytium formation. J. Virol. **75:**7351–7361.
42. **Ono, A., and E. O. Freed.** 2001. Plasma membrane rafts play a critical role in HIV-1 assembly and release. Proc. Natl. Acad. Sci. **98:**13925–13930.
43. **Ott, D. E.** 1997. Cellular proteins in HIV virions. Rev. Med. Virol. **7:**167–180.
44. **Pessin, J. E., and M. Glaser.** 1980. Budding of Rous sarcoma virus and vesicular stomatitis virus from localized lipid regions in the plasma membrane of chicken embryo fibroblasts. J. Biol. Chem. **255:**9044–9050.
45. **Pickl, W. F., F. X. Pimentel-Muinos, and B. Seed.** 2001. Lipid rafts and pseudotyping. J. Virol. **75:**7175–7183.
46. **Pitha, J., T. Irie, P. B. Sklar, and J. S. Nye.** 1988. Drug solubilizers to aid pharmacologists: amorphous cyclodextrin derivatives. Life Sci. **43:**493–502.
47. **Quigley, J. P., D. B. Rifkin, and E. Reich.** 1972. Lipid studies of Rous sarcoma virus and host cell membranes. Virology **50:**550–557.
48. **Renkonen, O., L. Kaarainen, K. Simons, and C. G. Gahmberg.** 1971. The lipid class composition of Semliki forest virus and plasma membranes of the host cells. Virology **46:**318–326.
49. **Root, M. J., M. S. Kay, and P. S. Kim.** 2001. Protein design of an HIV-1 entry inhibitor. Science **291:**884–888.
50. **Rothberg, K. G., Y. S. Ying, B. A. Kamen, and R. G. Anderson.** 1990. Cholesterol controls the clustering of the glycophospholipid-anchored membrane receptor for 5-methyltetrahydrofolate. J. Cell Biol. **111:**2931–2938.
51. **Rousso, I., M. B. Mixon, B. K. Chen, and P. S. Kim.** 2000. Palmitoylation of the HIV-1 envelope glycoprotein is critical for viral infectivity. Proc. Natl. Acad. Sci. USA **97:**13523–13525.
52. **Saphire, A. C., M. D. Bobardt, and P. A. Gallay.** 1999. Host cyclophilin A mediates HIV-1 attachment to target cells via heparans. EMBO J. **18:**6771–6785.
53. **Schaeffer, E., R. Geleziunas, and W. C. Greene.** 2001. Human immunodeficiency virus type 1 Nef functions at the level of virus entry by enhancing cytoplasmic delivery of virions. J. Virol. **75:**2993–3000.
54. **Scheiffele, P., A. Rietveld, T. Wilk, and K. Simons.** 1999. Influenza viruses select ordered lipid domains during budding from the plasma membrane. J. Biol. Chem. **274:**2038–2044.
55. **Simons, K., and J. Gruenberg.** 2000. Jamming the endosomal system: lipid rafts and lysosomal storage diseases. Trends Cell Biol. **10:**459–462.
56. **Simons, K., and E. Ikonen.** 2000. How cells handle cholesterol. Science **290:**1721–1726.
57. **Skehel, J. J., and D. C. Wiley.** 1998. Coiled coils in both intracellular vesicle and viral membrane fusion. Cell **95:**871–874.
58. **Slosberg, B. N., and R. C. Montelaro.** 1982. A comparison of the mobilities and thermal transitions of retrovirus lipid envelopes and host cell plasma membranes by electron spin resonance spectroscopy. Biochim. Biophys. Acta **689:**393–402.
59. **Smit, J. M., R. Bittman, and J. Wilschut.** 1999. Low-pH-dependent fusion of Sindbis virus with receptor-free cholesterol- and sphingolipid-containing liposomes. J. Virol. **73:**8476–8484.
60. **Thali, M., A. Bukovsky, E. Kondo, B. Rosenwirth, C. T. Walsh, J. Sodroski, and H. G. Gottlinger.** 1994. Functional association of cyclophilin A with HIV-1 virions. Nature **372:**363–365.
61. **Trono, D.** 1992. Partial reverse transcripts in virions from human immunodeficiency and murine leukemia viruses. J. Virol. **66:**4893–4900.
62. **Trono, D., M. B. Feinberg, and D. Baltimore.** 1989. HIV-1 Gag mutants can dominantly interfere with the replication of the wild-type virus. Cell **59:**113–120.
63. **Turelli, P., V. Doucas, E. Craig, B. Mangeat, N. Klages, R. Evans, G. Kalpana, and D. Trono.** 2001. Cytoplasmic recruitment of INI1 and PML on incoming HIV preintegration complexes: interference with early steps of viral replication. Mol. Cell **7:**1245–1254.
64. **Vincent, S., D. Gerlier, and S. N. Manie.** 2000. Measles virus assembly within membrane rafts. J. Virol. **74:**9911–9915.
65. **Wang, J. K., E. Kiyokawa, E. Verdin, and D. Trono.** 2000. The Nef protein of HIV-1 associates with rafts and primes T cells for activation. Proc. Natl. Acad. Sci. USA **97:**394–399.
66. **Weissenhorn, W., A. Dessen, S. C. Harrison, J. J. Skehel, and D. C. Wiley.** 1997. Atomic structure of the ectodomain from HIV-1 gp41. Nature **387:**426–430.
67. **White, J., and A. Helenius.** 1980. pH-dependent fusion between the Semliki Forest virus membrane and liposomes. Proc. Natl. Acad. Sci. USA **77:**3273–3277.
68. **Wild, C. T., D. C. Shugars, T. K. Greenwell, C. B. McDanal, and T. J. Matthews.** 1994. Peptides corresponding to a predictive alpha-helical domain of human immunodeficiency virus type 1 gp41 are potent inhibitors of virus infection. Proc. Natl. Acad. Sci. USA **91:**9770–9774.
69. **Zhang, J., A. Pekosz, and R. A. Lamb.** 2000. Influenza virus assembly and lipid raft microdomains: a role for the cytoplasmic tails of the spike glycoproteins. J. Virol. **74:**4634–4644.
70. **Zheng, Y. H., A. Plemenitas, T. Linnemann, O. T. Fackler, and B. M. Peterlin.** 2001. Nef increases infectivity of HIV via lipid rafts. Curr. Biol. **11:**875–879.